Control of Porosity on Durability of Limestone at the Great Sphinx, Egypt

ADINARAYANA R. PUNURU, AHAD N. CHOWDHURY, NIRAJ P. KULSHRESHTHA, and K. L. GAURI
Department of Geology
University of Louisville
Louisville, Kentucky 40292, U.S.A.

ABSTRACT / The study of the porosimetric data obtained from intrusion, extrusion, and reintrusion of mercury in limestone samples from the region of the sphinx reveals the characteristics of the pore system and allows analysis of durability factors.

The pore system in all these rocks consists of "ink-bottle" pores. As the initial intrusion and extrusion have been completed, some mercury always remains in the sample. This trapped mercury represents the volume of large voids of the ink-bottle pore system. The distribution of the volume of the narrow throats of this system is revealed by the reintrusion curves.

The curves obtained by plotting extrusion and reintrusion volumes against corresponding pressures enclose a loop. These curves relate to pore throats only. As entrapment of mercury does not occur in these pores, their distribution frequency and sorting seem to cause this hysteresis.

The pressure/volume data also have been interpreted in terms of work needed to inject and extrude mercury from the pores. This thermodynamic analysis of the data has provided an additional, although less well-defined, means to characterize the porous stones.

We have used in this study the model-dependent pore-size distributions and model-independent thermodynamic properties to develop durability factors. The factors based upon the combination of pore sizes in the range of <0.5, 0.5–5, and >5 μm precisely fit the observed durability of limestones at the sphinx, some of which have been exposed for more than 5,000 yr to the ambient atmosphere.

Introduction

The durability of stone is largely controlled by the pore-size distributions. To obtain these quantitatively (Dullien and Batra 1970) by microscopic means is not only cumbersome but nearly impossible, particularly due to the intricate network of fine pores that are difficult to reconstruct three-dimensionally. Mercury-intrusion porosimetry consists of injecting, under pressure, mercury, a non-wetting liquid, into pores. The size of the pores intruded by mercury depends upon the amount of the applied pressure, but to calculate the pore radii a configuration of pores must be assumed. The classical Washburn (1921) equation, assuming the pores being cylindrical, expresses the relationship as follows:

$$r = -(2\gamma \cos\theta)/P \qquad (1)$$

where r = pore radius, in μm; γ = surface tension, 485 dynes/cm; θ = contact angle of mercury with stone surface, 130°; P = applied pressure, in psi.

In a pore system where large and small pores are interconnected, the pressure/volume curves do not show the large pores directly. The reason is that a small connecting pore will allow the entry of mercury into a large pore at the pressure adequate for the breakthrough of this small pore. If a large pore is connected to small pores of variable sizes, then, upon increasing pressure, the largest of connecting pores will control the entry of mercury into the large pore. As a result, the large pores become masked in normal mercury-intrusion data. However, the pressure/volume (PV) curves for initial intrusion, extrusion, and reintrusion allow delineation of such interconnected large and small pores.

Besides pore-size distributions, the PV data can also be used to calculate the work expended during the injection and withdrawal of mercury. This work is a model-independent quantity and offers an additional method to characterize the building stone.

Several efforts have been made in the past to rank stones for durability on the basis of their pore characteristics. Kaneuji (1978) developed a ranking scheme based upon the total pore volume and median pore diameter for certain Indiana limestones. Our analysis of the pore-size distributions has allowed us to develop a durability equation, which, when applied to ancient as well as modern well-known building stones, represents accurately their weathering behavior. The results

The present address for A. R. Punuru is Link-Miles Simulation Corporation, 8895 McGaw Road, Columbia, MD. The present address for A. N. Chowdhury is Kentucky Division of Water Management, 18 Reilly Road, Frankfort, KY, and the present address for N. P. Kulshreshtha is Jefferson Regional Laboratory, 3600 Chamberlain Lane, Louisville, KY.

of this study are particularly useful in the selection of stone for restoration of many decaying monuments in Egypt.

Materials and Methods

The limestone samples were obtained from the core of the sphinx (Fig. 1) and from the corresponding rock units extending into the walls of the sphinx sanctuary. The samples were extracted from some depth into the strata in an effort to exclude the weathered portion of stone as far as possible. The samples for the porosimeter were nearly quarter-inch-long cylinders with a diameter somewhat less than the length. The surface of the samples was polished with 600-grit carbide powder, cleaned in an ultrasonic bath for a few seconds, dried at 100°C, and then cooled in a desiccator to room temperature.

A Micromeritics Pore-Sizer 9300 was used to obtain intrusion, extrusion, and reintrusion data in the pressure range of 5–30,000 psi. The intrusion and extrusion volumes of mercury were measured in terms of capacitance as picofarads converted to cubic centimeters per gram of sample, using conversion factors given for respective penetrometers by the manufacturer. Adequate time was allowed to achieve a steady state of mercury penetration and ejection. The experiment on a sample sometimes lasted three days.

The data collected from the Pore-Sizer 9300 were stored on a computer disk. The cumulative pore-volume and pore-size distribution curves were drawn using the Dec-graph program on a Vax computer.

Discussion

Scanning electron microscopy (Chowdhury and others 1990) has clearly revealed that the sphinx limestones have "ink-bottle" pores (Fig. 2). In such a system of pores, large voids are commonly connected to each other through narrow throats. We will attempt in the following pages to determine the correlatives of these pores in the pressure/volume data obtained from mercury-intrusion porosimetry.

In the prevailing ink-bottle pore configurations, the narrow throats limit the movement of mercury into the large cavities, so that at lower pressures the mercury is unable to penetrate the corresponding large pores. These become filled later when the pressure for the breakthrough of the narrow throat has been achieved. In fact, the largest of the throats controls the filling of the large pores because, once mercury begins to flow into a large pore, a steady state of intrusion volume must be achieved in the experimental procedure before a switch is made to the next higher pressure, indicating a narrower pore. Consequently, the

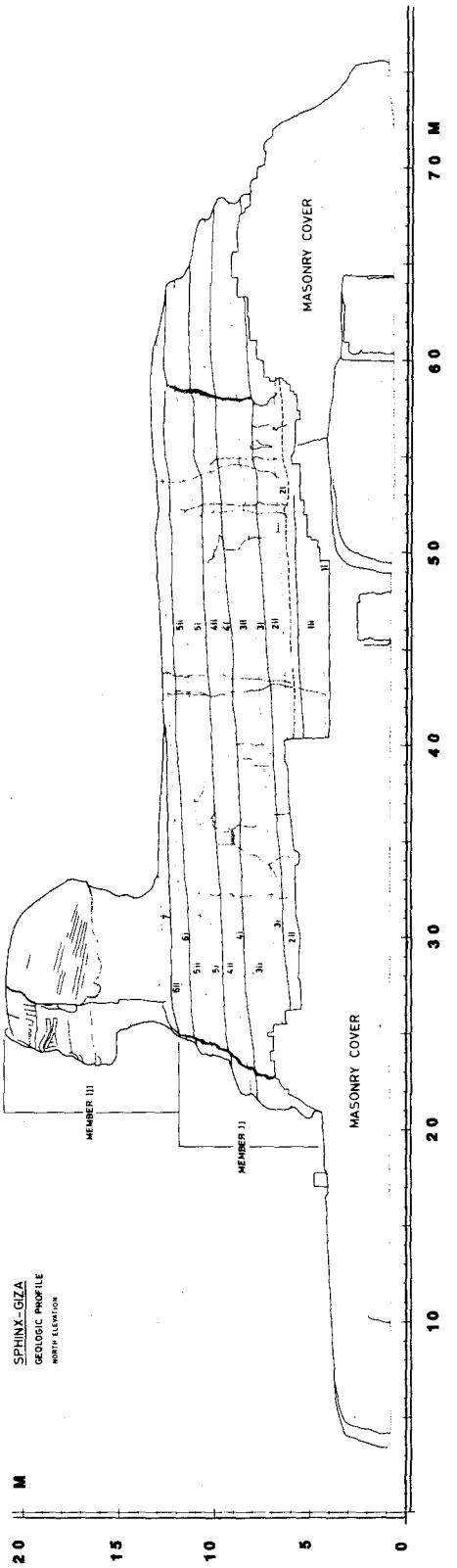

Figure 1. Geologic profile of the sphinx showing the beds (1–7) of the thorax.

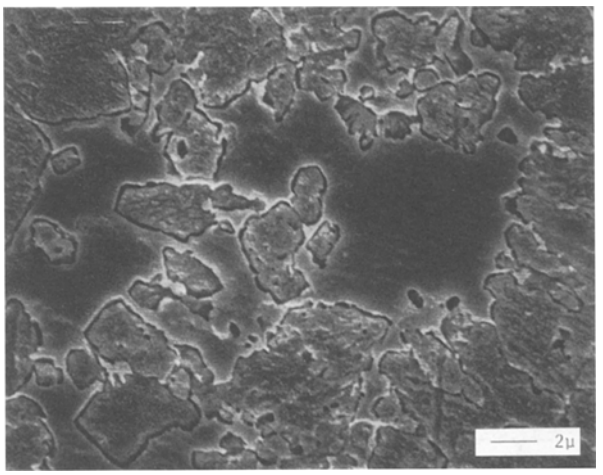

Figure 2. Micrograph of epoxy impregnated sample from bed 6ii (see Chowdhury and others 1990) showing ink-bottle pores. The cavities here are large pores and the connecting throats represent capillaries, i.e., small pores, of up to 5 μm diameter.

volume/pore-size curves representing first intrusion mask the presence of the large pores even though the total volume of the intruded mercury—thus the total porosity—is accurately revealed. These curves must then be deconvoluted in order to gain an insight into the presence and distribution of the large pores. The first of these objectives, i.e., the identification of large pores and their volume, has been achieved by studying the hysteresis generated in the process of initial intrusion and extrusion of the mercury. A way to determine the distribution of large pores has not yet been found, however.

The volume of the extruded mercury in all studied samples is less than that of the total intruded mercury. Obviously, in the depressurizing mode, the narrow throats of the ink-bottle pores do not, at pressures below their breakthrough pressure, allow the mercury to be extruded from the large pores (Wardlaw 1976; Wardlaw and Taylor 1976; Wardlaw and McKellar 1981). The trapped volume thus represents the space occupied by pores larger than those revealed directly by the initial intrusion in the volume/pore-size curves (Figs. 3 and 4). These large pores are seen as vugs in the scanning electron microscopy (Fig. 2).

The second intrusion takes place entirely in the throats of the ink-bottle pores only, because the large cavities had remained filled with the mercury during the extrusion process. The second intrusion then gives the true volume and the distribution of the throat sizes. The PV curves resulting from extrusion and the second intrusion enclose a hysteresis loop. This loop entails relationships between various sizes of throat interconnection without any entrapment of the mercury. Relevant porosimetric data from the limestone beds of the thoracic region of the sphinx are shown in Figure 3. These curves clearly reveal the distinction between the bottom and top portions of a bed and between the lower and the upper beds (Gauri and Holdren 1981; Chowdhury and others 1990). The top portion of a bed with respect to its bottom portion and the upper beds, in general, have a larger volume of the large pores (vugs), have widely scattered throat sizes, and possess lower hysteresis energy calculated on the basis of PV work of extrusion and reintrusion.

Robertson (1982, and several private communications) and Lowell and Shields (1981) have suggested that the hysteresis loop may have been generated because of the change in the contact angle (θ) of mercury from the forward to the backward movement attending the respective intrusion and the extrusion of the mercury. However, the shape of these loops, the area they enclose, and their gradient in the PV diagram change systematically from the lower to the upper layers of the sphinx strata. Furthermore, even if two strata receive the same volume of injected mercury, their hysteresis loops may be different. This leads to the suggestion that the influence of the pore system over the movement of the mercury is very large indeed, even though the change in the contact angle may have contributed to this hysteresis.

The durability of stone in natural exposure is normally related to the movement of water through pores, which, in turn, is controlled by the pore-size distributions. In his classic work Schaffer (1932, facsimile reprinted 1972) showed that among Portland stones those most affected by the crystallization test had high microporosities. Honeyborne and Harris (1958) gave an empirical criterion of durability: stone in which at least 70 percent of the porosity was present in the form of pores greater than 5 μm in diameter. In the following discussion of the ink-bottle pores, the throat sizes less than 0.5 μm in diameter are termed small capillaries and those between 0.5 and 5 μm are termed large capillaries. All cavities larger than 5 μm are termed large pores.

In cold climates, freezing of water in the pore space may damage the stone. In hot and arid climates, crystallization of salts produces similar, although more damaging, effects. Those rocks that readily become critically saturated, i.e., in which the entire pore space becomes completely filled with water (Table 1, lower beds) suffer maximum damage. This condition is easily attained in a stone possessing a large volume of small capillaries. Here, the strong capillary suction fills all the pores completely. As the crystallization begins, first in the large pores (Everett 1961), presumably hydrostatic pressure is generated, acting against the pore

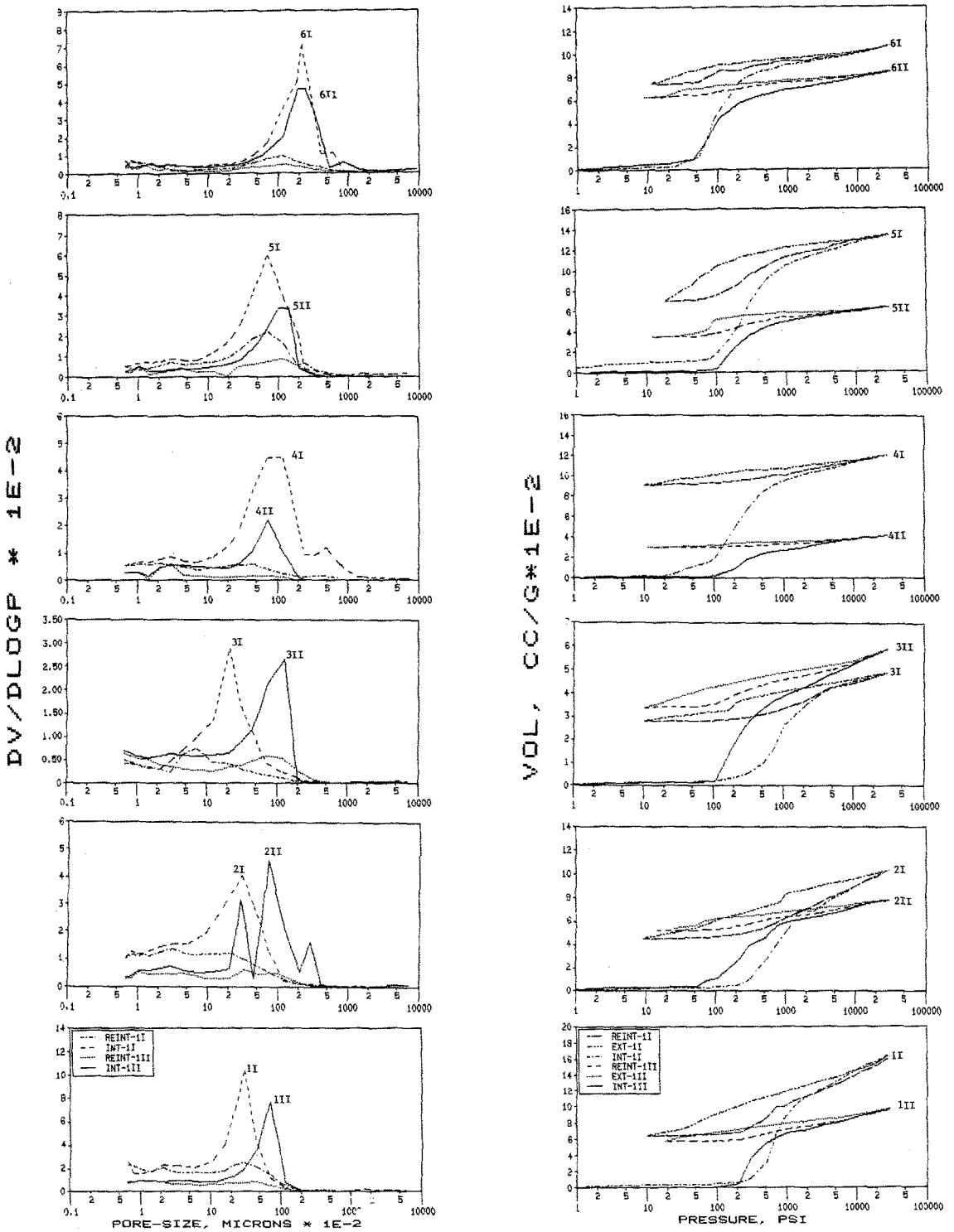

Figure 3. Porosimetry of sphinx limestones: Specimens 1–6 are from the beds shown in Figure 1. Specimens of bed 7 are shown in Figure 4. **A.** Pore-size distributions showing that the lower portion of each bed has a maximum of capillaries of smaller diameter than the upper portion of the same bed. Also, the upper beds have larger capillaries than the lower beds. **B.** PV curves showing, among other features, the volume of mercury trapped in the pores. For example the trapped mercury in sample 1i is nearly 40 percent, and in 6i it is nearly 75 percent. This trapped volume represents the volume of large pores.

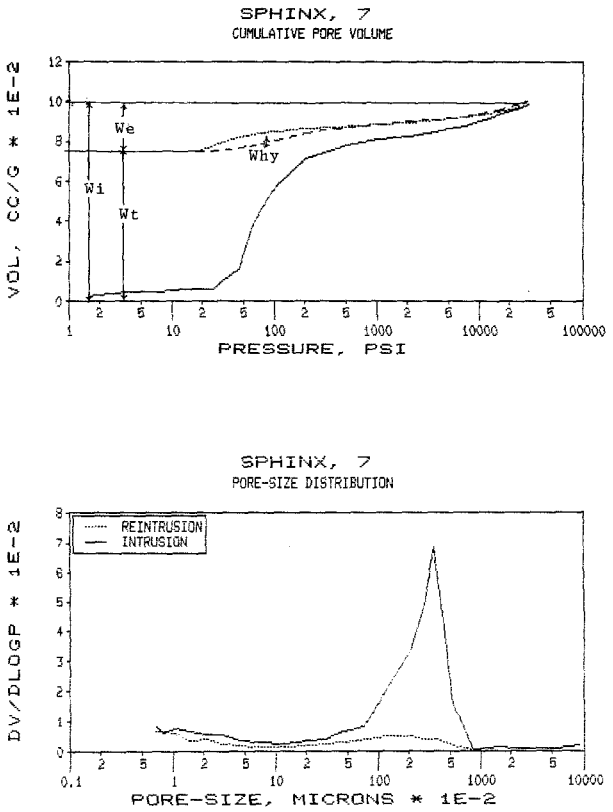

Figure 4. Porosimetry of bed 7, also showing the areas of PV work used in the thermodynamic analysis of the porosimetric data (Table 3).

Table 1. Saturation coefficient of sphinx thorax beds[a]

Sample	Saturation coefficient
7	0.83
6ii	0.82
6i	0.94
5ii	0.93
4ii	0.91
4i	0.89
3ii	0.96
2ii	0.95
1ii	1.00
1i[b]	0.77

[a]Saturation coefficient is the ratio of water absorbed by capillarity to the water absorbed under pressure.
[b]Samples disintegrate when immersed in water.

walls. Eventually, the elastic modulus of the stone is overcome (Cassaro and others 1982), and the stone succumbs by disintegration. On the other hand, stones possessing large capillaries have weaker suction. Furthermore, the presence of the large volume of large pores in such samples allows the pores to be only partially filled. The hydrostatic pressure generated on crystallization in such cases is unable to act upon the pore wall, and the stone escapes disintegration. With this background, the following features have been found to influence the durability of the sphinx rocks:

1. Presence of a large volume of narrow capillaries (<0.5 μm) is detrimental in any case. The strong suction by these narrow capillaries fills all the pores after water has become available in the environment of the stone. The durability may somewhat increase if large pores are present, but even these pores may become readily filled with the water supplied by the narrow capillaries. The specimens from beds 1–3 in the sphinx sequence belong to this category. They possess a saturation coefficient approaching the value of 1, suggesting that empty space does not exist in these rocks and that crystallization pressure may be released. These rocks have suffered maximum deterioration in the field.
2. Limestones with abundant large capillaries (0.5–5 μm) are generally more durable, as large capillaries exert a weaker suction. Because of this, the large pores do not seem to become entirely filled with water (Table 1), and adequate space remains for the release of the crystallization pressure.
3. As a corollary of 1 and 2 above, a relatively larger volume of the pore space occupied by the large pores will enhance the stone's durability. This is clearly seen in the upper beds of the rock sequence exposed at the sphinx.

Durability Factors

Kaneuji (1978) and Kaneuji and others (1980), developed durability factors for certain crushed Indiana limestones used as aggregates in the manufacture of concrete for pavements. These factors were based upon the freeze–thaw tolerance of aggregate and its correlation with the porosity characteristics of the aggregate as expressed below:

$$EDF = K_1/PV + K_2\,(MD) + K_3$$

where EDF = expected durability factors; PV = intruded pore volume of pores larger than 0.0045 μm in diameter, expressed in cc/g; MD = median diameter of pores larger than 0.0045 μm; K_1, K_2, and K_3 are constants with values of 0.579, 6.24, and 3.04, respectively.

The stones possessing an EDF value of 50 or higher were designated as durable against frost weathering. The pores considered by Kaneuji include both our

narrow and large capillaries. An estimation of the large pores in Kaneuji's material cannot be made because he did not determine the extrusion and reintrusion volumes, but he must have been aware of the presence of the ink-bottle pores, as he suggested that the pores larger than those included in his calculations would only increase the *EDF* values of the durable stones.

The application of Kaneuji's equation to our porosimetric data reveals a vague correspondence of the calculated *EDF* values to the observed durability. In light of present study, which has suggested that three pore types are influential in determining the durability of the sphinx rocks, we have developed new relationships that accurately describe these rocks.

Durability Factors for Sphinx Limestones

The durability factors have been calculated from the relative volume of pores shown in Table 2. The durability factors equation is given below:

$$DF = A_1 \times V_1 + A_2 \times V_2 + A_3 \times V_3 \qquad (2)$$

where V_1, V_2, and V_3 are percentage pore volumes in the pore ranges of >5, 0.5–5, and <0.5 μm, respectively. A_1, A_2, and A_3 are constants with the values 1.2338, 2.6220, and −0.9841, respectively.

The values of the constants were calculated from the solution of three simultaneous equations in which the pertinent properties of three samples, one each from beds 7, 6ii, and 6i, were assigned durability values of 100, 98, and 95, respectively. All these stones appear to be in a fair state of preservation. Table 2 shows the durability factors of the strata forming the sphinx core, as well as of some Pharaonic veneer stones that are excellently preserved despite their 5,000 yr of exposure to local conditions. Durability factors have also been calculated for Indiana limestone, a common building stone of proven quality in the United States. These calculated factors match the observed durability as well as the durability inferred from the petrographic properties of the rock (Gauri 1984).

Theoretical Background of Thermodynamic Analysis of Mercury Porosimetry Data

In mercury porosimetry, work is performed during the processes of initial intrusion (W_i), extrusion (W_e), and reintrusion (W_{re}) (Fig. 3), given by the general relationship

$$dW = PdV \qquad (3)$$

In fact, the Washburn equation (1), fundamental in mercury porosimetry, is derived from the work-related Young and Dupre's equation

$$W = -(\gamma_{LV} \cos \theta)\, \Delta A \qquad (4)$$

where ΔA is the change in the area of the capillary wall in a rising or depressing liquid in a capillary. However, in a column with a volume V, subjected to a pressure, P, above ambient,

$$W = \Delta PV \qquad (5)$$

Combining equations 4 and 5,

$$\Delta PV = -(\gamma \cos \theta)\, \Delta A \qquad (6)$$

For a circular capillary, the terms V and ΔA are given by $\pi r^2 l$ and $2\pi rl$, respectively. Substituting these values in equation 6, gives the Washburn equation, restated

$$\Delta P\, r = -2\, \gamma \cos \theta \qquad (1)$$

Equations 6 and 1 are identical, but the latter represents cylindrical pores only. However, for any other shape of pores, equation 6 becomes the operating equation. The thermodynamic work thus may be considered as a model independent quantity.

The purpose of the following discussion is to present the PV work as an additional means to characterize stones. Our treatment of the subject follows the lead of Robertson (1982), who has studied Portland stones from different quarries with a view of selecting durable stone for the restoration of Westminster Abbey, and the work of Lowell and Shields (1981, 83, 84) concerning the theory and practice of thermodynamics in mercury porosimetry.

Thermodynamic Analysis of Sphinx Porosimetric Data

The work of intrusion, extrusion, and reintrusion was calculated by dividing the area above respective PV curves into n intervals, based upon the pressures at which the corresponding volumes were determined. The integral work of W_i, W_e, and W_{re} are given by

$$W_i = \Sigma \overline{P} \Delta V_i \qquad (7)$$

$$W_e = \Sigma \overline{P} \Delta V_e \qquad (8)$$

$$W_{re} = \Sigma \overline{P} \Delta V_{re} \qquad (9)$$

where ΔV_i, ΔV_e, and ΔV_{re} are the volume changes in an interval j and $j + 1$ and $\overline{P}$ is the average pressure in that interval.

Alternatively, W_i may be considered graphically (Fig. 4) as consisting of three parts, namely work of entrapment (W_t), work of hysteresis loop (W_{hy}), and work of extrusion (W_e), expressed as

$$W_i = W_t + W_{hy} + W_e \qquad (10)$$

These may be independently evaluated from the PV data. The amount of work calculated by these various

Table 2. Durability factors (*DF*) calculated on basis of pore-size distributions

Sample	Total pore volume (%) V_1 (>5 μm)	V_2 (0.5–5 μm)	V_3 (<0.5 μm)	*DF*
7	74.68	9.09	16.23	100.0
6ii	74.59	8.84	16.57	98.9
6i	69.30	11.25	19.54	95.8
5ii	55.00	19.12	25.88	92.5
5i	52.11	18.77	29.12	84.9
4ii	74.88	5.03	20.09	85.8
4i	71.49	4.34	24.17	75.8
3ii	57.56	13.04	29.40	76.3
3i	57.23	3.70	39.07	41.9
2ii	66.01	8.04	25.95	76.9
2i	43.86	3.32	52.82	10.8
1ii	63.28	4.00	32.72	56.4
1i	40.69	5.50	53.81	11.7
SW16	64.50	11.50	23.90	86.2
SW16	61.20	12.50	26.30	82.4
T22	49.68	24.65	25.66	100.7
T22	53.44	19.59	26.98	96.8
INDY1	51.54	27.36	21.10	114.6
INDY2	52.39	21.38	26.32	94.5
INDY3	61.84	14.59	23.57	91.4

Table 3. PV work calculated from porosimetry data

Sample[a]	W_i (J/g)	Percent of W_i W_t	W_{hy}	W_e	W_t/W_{hy}
7	1.387	26.74	15.82	57.44	1.69
6ii	1.075	36.22	8.30	55.48	4.36
6i	1.152	11.70	12.90	75.30	0.91
5ii	0.878	23.84	11.85	64.33	2.02
5i	1.690	31.07	17.26	51.67	1.80
4ii	0.747	25.45	3.97	70.57	6.10
4i	1.515	24.42	18.83	56.75	1.30
3ii	1.294	21.44	14.07	64.47	1.52
3i	1.000	15.00	31.00	54.00	0.48
2ii	1.168	22.00	26.14	51.86	0.84
2i	2.783	12.77	38.86	48.36	0.33
1ii	1.926	12.75	24.59	62.66	0.52
1i	4.419	7.37	11.38	81.25	0.64
SW16	1.146	17.80	47.20	35.00	0.38
SW16	2.126	21.70	11.20	67.10	1.94
T22	1.067	51.17	33.79	15.04	1.51
T22	1.010	28.63	38.18	33.19	0.75
INDY1	1.076	18.4	12.95	68.65	1.42
INDY2	1.121	7.18	8.61	84.21	0.83
INDY3	1.616	47.63	7.50	44.87	6.35

[a]Samples 1–7 are from the core of the sphinx. SW16 and T22 are from veneer stones used in the pharaonic restoration. INDY 1–3 are samples from Indiana limestones.

means coincides, owing to their same origin. The data obtained by the application of equation 10 are given in Table 3. The following features are readily apparent from this analysis:

1. The work of entrapment is higher for the upper beds of the sphinx than for the lower beds. Furthermore, the upper portion of a bed shows more work than its lower portion. This result corresponds with the preceding study based upon pore-size distributions, where it is

seen that the large pores, which are responsible for the entrapment of mercury, are more abundant in the upper strata.

2. The work of extrusion is higher for the lower beds. This correlates well with the larger microporosity of these beds.
3. The work of the hysteresis loop does not show a definite trend, but a correlation between the ratio of hysteresis and entrapment energies and the observed durability is apparent in that the lower beds possess lower W_t/W_{hy} values than the upper beds.
4. Other studied limestones, namely, the Pharaonic veneer stones and the Indiana limestone do not fit the above schemes rigorously. Work is in progress to deal with these matters in greater detail.

Conclusion

Schaffer (1931) wrote, "In a series of nearly 100 quarry samples recently examined, measurement of total porosity proved useless as a basis of classification, but measurement of the microporosity, measured by the physical method [i.e., capillary suction] was found to afford a method of classification into tolerably well-defined groups." Schaffer, comparing his work to Scott Russell's (quoted as private communication) separated micro- and macroporosity by a pore size of 5 μm diameter. Modern, precise measurements, by mercury porosimetry, of porosity in an indefinite range of pore sizes, has enabled us to develop a reasonably accurate rating system. It is hoped that continuing work on this aspect and the thermodynamic fundamentals of the free energy in pores will permit an additional, perhaps a universally applicable, system of selecting durable stones.

References Cited

Cassaro, M. A., K. L. Gauri, M. Sharifinassab, and A. Sharifian, 1982, On the strength and deformation properties of Indiana limestone and concrete in presence of salts; *in* K. L. Gauri and J. A. Gwinn, eds., Fourth international congress on deterioration and preservation of stone objects: University of Louisville, Louisville, KY, p. 57–76.

Chowdhury, A. N., A. Punuru, and K. L. Gauri, 1990, Weathering of limestone beds at the Great Sphinx: Environmental Geology and Water Science, v. 15, pp. 217–223.

Dullien, F. A. L., and V. K. Batra, 1970, Determination of structure of porous media; *in* R. J. Nunge, ed., Flow through porous media: American Chemical Society, Washington, D.C., p. 1–30.

Everett, D. H., 1961, The thermodynamics of frost damage to porous solids: Transactions of the Faraday Society, v. 57, p. 1541–1557.

Gauri, K. L., 1984, Geologic study of the sphinx: American Research Center in Egypt, Newsletter, 127, p. 19–27.

Gauri, K. L., and G. C. Holdren, 1981, Deterioration of the stone of the Great Sphinx: American Research Center in Egypt, Newsletter, 114, p. 35–47.

Honeyborne, D. B., and P. B. Harris, 1958, The structure of porous building stone and its relation to weathering behavior: Proceedings, 10th symposium of the Colston research society, Butterworths Scientific Publications, London, p. 343.

Kaneuji, M., 1978, Correlation between pore size distribution and freeze thaw durability of coarse aggregate in concrete: Report JHRP-IN-78-15, Joint Highway Research Project, Purdue University, Reproduced by the National Technical Information Service. U.S. Department of Commerce, Springfield, VA 22161, p. 142.

Kaneuji, M., D. N. Winslow, and W. L. Dolch, 1980, The relationship between an aggregate's pore size distribution and its freeze thaw durability in concrete: Cement and Concrete Research, v. 10, p. 433–441.

Lowell, S., and J. E. Shield, 1983, Hysteresis, entrapment and wetting angle in mercury porosimetry: Journal of Colloid and Interface Science, v. 83, p. 273–278.

Lowell, S., and J. E. Shield, 1984, Powder surface area and porosity; *in* B. Scarlett, ed., Powder technology series, 2nd ed., Chapman & Hall, New York, 234 p.

Lowell, S., and J. E. Shields, 1981, Influence of contact angle on hysteresis in mercury porosimetry: Journal of Colloid and Interface Science, v. 80, p. 192–196.

Robertson, W. D., 1982, Evaluation of the durability of limestone masonry in historic buildings; *in* K. L. Gauri and J. A. Gwinn, eds., Fourth international congress on deterioration and preservation of stone objects: University of Louisville, Louisville, KY, p. 261–278.

Schaffer, R. J., 1932, The weathering of natural stones: Department of Scientific and Industrial Research special report, 18, Reprinted by the Building Research Establishment (1972): Garston Watford, WO27JR, England, 149 p.

Wardlaw, N. C., 1976, Pore geometry of carbonates as revealed by pore casts and capillary pressure data: American Association of Petroleum Geologists Bulletin, v. 60, p. 245–257.

Wardlaw, N. C., and M. McKellar, 1981, Mercury porosimetry and the interpretation of pore geometry in sedimentary rocks and artificial models: Powder Technology, v. 29, p. 127–143.

Wardlaw, N. C., and R. P. Taylor, 1976, Mercury capillary pressure curves and the interpretation of pore structure and capillary behavior in reservoir rocks: Bulletin Canadian Petroleum Geologists, v. 24, p. 225–262.

Washburn, E. W., 1921, Note on a method of determining the distribution of pore sizes in a porous material: Proceedings of the National Academy of Sciences of the United States of America, v. 7, p. 115–116.